# Supplementary Materials

## Tenascin C protects aorta from acute dissection in mice

Taizo Kimura [1,2,3], Kozoh Shiraishi [2], Aya Furusho [4], Sohei Ito [4], Saki Hirakata [4], Norifumi Nishida [4], Koichi Yoshimura [1,5], Kyoko Imanaka-Yoshida [6,7], Toshimichi Yoshida [6,7], Yasuhiro Ikeda [1,2], Takanobu Miyamoto [4], Takafumi Ueno [4], Kimikazu Hamano [5], Michiaki Hiroe [8], Kazutaka Aonuma [3], Masunori Matsuzaki [1,2], Tsutomu Imaizumi [4], Hiroki Aoki [1,4*]

1 Department of Molecular Cardiovascular Biology, Yamaguchi University School of Medicine.

2 Division of Cardiology, Department of Medicine and Clinical Science, Yamaguchi University Graduate School of Medicine.

3 Division of Cardiovascular Medicine, Medical Science for Control of Pathological Processes, Graduate School of Comprehensive Human Science, University of Tsukuba.

4 Cardiovascular Research Institute, Kurume University.

5 Department of Surgery and Clinical Science, Yamaguchi University Graduate School of Medicine.

6 Department of Pathology and Matrix Biology, Mie University Graduate School of Medicine.

7 Mie University Research Center for Matrix Biology, Mie University Graduate School of Medicine.

8 National Center for Global Health and Medicine, Tokyo, Japan.

**Supplementary Figure 1.** Effects of Ca+AngII treatment.
(**a**) Images of EVG staining of the infrarenal aortae of wild type (WT) and TNC-KO (KO) mice with the indicated treatment. (**b**) Diameters of infrarenal aortae from WT or TNC-KO mice with the indicated treatment. The number of animals are indicated in parentheses. (**c**) Systolic blood pressure in WT (open circles) and TNC-KO (closed circles) mice before and after the Ca+AngII treatment. Data are shown as mean ± SD.

**Supplementary Figure 2.** AAD in TNC-KO mice.
(**a**) Representative ultrasonographic image of an enlarged aorta in TNC-KO mice. Bars, 0.5 mm. (**b**) Images of EVG staining of AAD in TNC-KO mice 6 weeks after Ca+AngII treatment. Insets are enlarged images of the rectangles in the upper panels and show disrupted elastic lamellae (arrows). The true lumen (tr) and the false lumen (fl) of the aorta are indicated.

**Supplementary Figure 3.** Cytokine profile of mice treated with AngII or Ca+AngII.
Quantitative analysis of cytokines (Bio-plex, Bio-Rad) in the sera of mice without (Cont, n = 4) and with AngII (n = 5) or Ca+AngII (n = 8) treatment. Data are shown as mean ± SD.

**Supplementary Figure 4.** Physiological measurements in live mice.
(**a**) Blood pressure measurements by aortic catheterization at various positions in aortae as illustrated at the bottom of the panel. Mice were untreated (open circles) or treated with Ca (closed circles), AngII (open squares), or Ca+AngII (closed squares) for 1 week. Data are the mean ± SD of eight independent observations. Systolic blood pressures were deliberately adjusted to approximately 100 mmHg for the measurement of dP/dt as shown in Figure 2. (**b**) The descent rates of the anterior aortic walls as determined by ultrasonography in live mice with no treatment (open columns) and Ca+AngII treatment for 1 week (closed columns). Data (% end diastolic diameter/sec) are the mean ± SD of six independent observations. *$P < 0.05$ and ***$P<0.001$ as compared to control (Cont).

**Supplementary Figure 5.** TNC expression in aorta treated with AngII or Ca+AngII.
(**a**) β-galactosidase staining of aortae from *Tnc* reporter mice 0 (Cont), 4 or 6 weeks after starting the indicated treatment. Note that $CaCl_2$-treated infrarenal aortae

(brackets) developed fibrosis that interfered with penetration of the chromogenic substrate and thus with color development. (**b**) Cross-sectional images of the aorta 4 weeks after the Ca+AngII treatment. The tissues were stained for β-galactosidase activity (βgal), smooth muscle α-actin (αSMA) and hematoxylin (Nuclei). Bar, 50 $\mu$m. (**c**) Serum levels of TNC are shown. Data are mean ± SD of five independent observations for each group. *P < 0.05 compared to control (Cont).

**Supplementary Figure 6.** Transcriptome of the suprarenal aorta before AAD onset. Functional annotation clusters obtained by DAVID are shown as heat maps of the average linkage hierarchical clustering with the corresponding gene symbols of subclusters. Functional annotation clusters are shown in the order of the enrichment scores from panels (**a**) to (**d**).

**Supplementary Figure 7.** Gene expression profile of aortae and smooth muscle cells. (**a**) Induction of a panel of proinflammatory genes in the suprarenal aorta was analyzed by quantitative RT-PCR using the $RT^2$ Profiler PCR Array System (SA Biosciences, PAMM-077). Total RNA samples were obtained from the suprarenal aortae of WT mice (blue bars) or TNC-KO mice (red bars) after 1 week of Ca+AngII treatment. Data are the mean ± SD of eight independent observations and are expressed as the log ratio of induction from baseline. Data are plotted in order from greatest to least induction in TNC-KO mice. (**b**) The same set of genes as in (**a**) were analyzed in TNC-KO aortic smooth muscle cells (SMC) cultured in the presence (blue bars) or absence (red bars) of exogenously added TNC (10 $\mu$g/mL). Induction of the genes by 10 ng/mL TNFα are shown as the mean ± SD of four independent observations and are shown as log ratios. (**c**) Induction of collagen family genes was analyzed using GeneChip (Mouse Genome 430 2.0, Affymetrix) in the samples in (**b**). Genes with the detection call "absence" in all samples were omitted. Data are plotted in order of greatest to least induction in aortic SMC in the absence of exogenous TNC for (**b**) and (**c**).

**Supplementary Figure 8.** Histological analyses of aortae from WT or TNC-KO mice with or without 1 week of Ca+AngII treatment. (**a**) Representative images of picrosirius red staining of aortae are shown. Branches (br) were excluded from the analysis. (**b**) Quantitative analysis of adventitial sirius red staining is shown. Animal numbers are

indicated in parentheses. (**c**) Representative images of immunohistochemical stainings are shown for type I collagen, lysyl oxidase and fibronectin. Bars, 200 $\mu$m.

**Supplementary Figure 9.** Imaging cytometric analysis for cell populations. Aortae were obtained from WT or TNC-KO mice with or without 1 week of Ca+AngII treatment. The number of animals are indicated in parentheses. Subpopulation without αSMA staining was analyzed for CD45 expression in the aortic tissue sections.

**Supplementary Figure 10.** Imaging cytometric analyses for NFκB, phospho-Stat3 (P-Stat3) and phospho-Smad2 (P-Smad2) are shown for total populations and subpopulations with or without αSMA expression from the same dataset for Figure 5a. Blue and red lines indicate the histograms of WT and TNC-KO, respectively. Gray arrows indicate the changes in cell populations in TNC-KO.

**Supplementary Movie 1.** OCT imaging of AAD in mice.
A series of optical sections obtained by optical coherence tomography (OCT) of an enlarged aorta from a Ca+AngII-treated TNC-KO mouse. The aorta was scanned from the distal to the proximal portion, and the scans spanned the enlarged region.

**Supplementary Movie 2.** Three-dimensional reconstruction of OCT images.
3D reconstruction of a mouse AAD from a series of OCT images using OsiriX Imaging Software (version 5.0).

**External Databases 1.** The dataset for transcriptome analysis.
The dataset for the transcriptome analysis can be found in Gene Expression Omnibus at the following link:
http://www.ncbi.nlm.nih.gov/geo/query/acc.cgi?token=fxgvrosykcciedq&acc=GSE36899

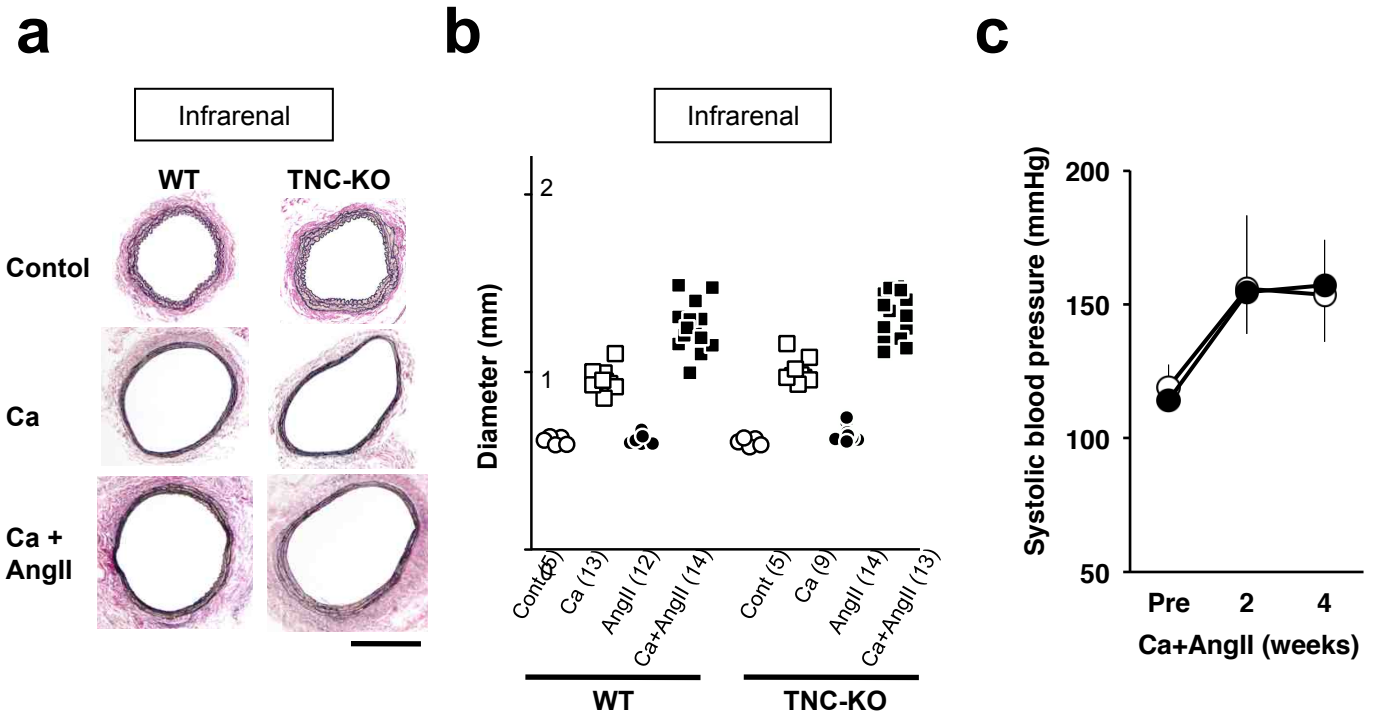


**Supplementary Figure 1**

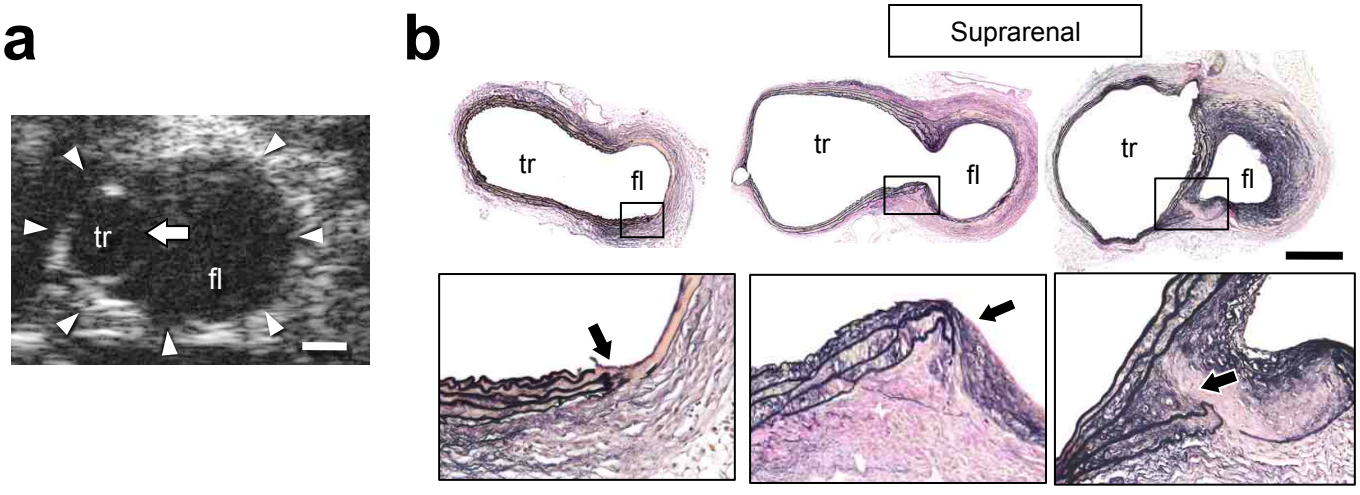


**Supplementary Figure 2**

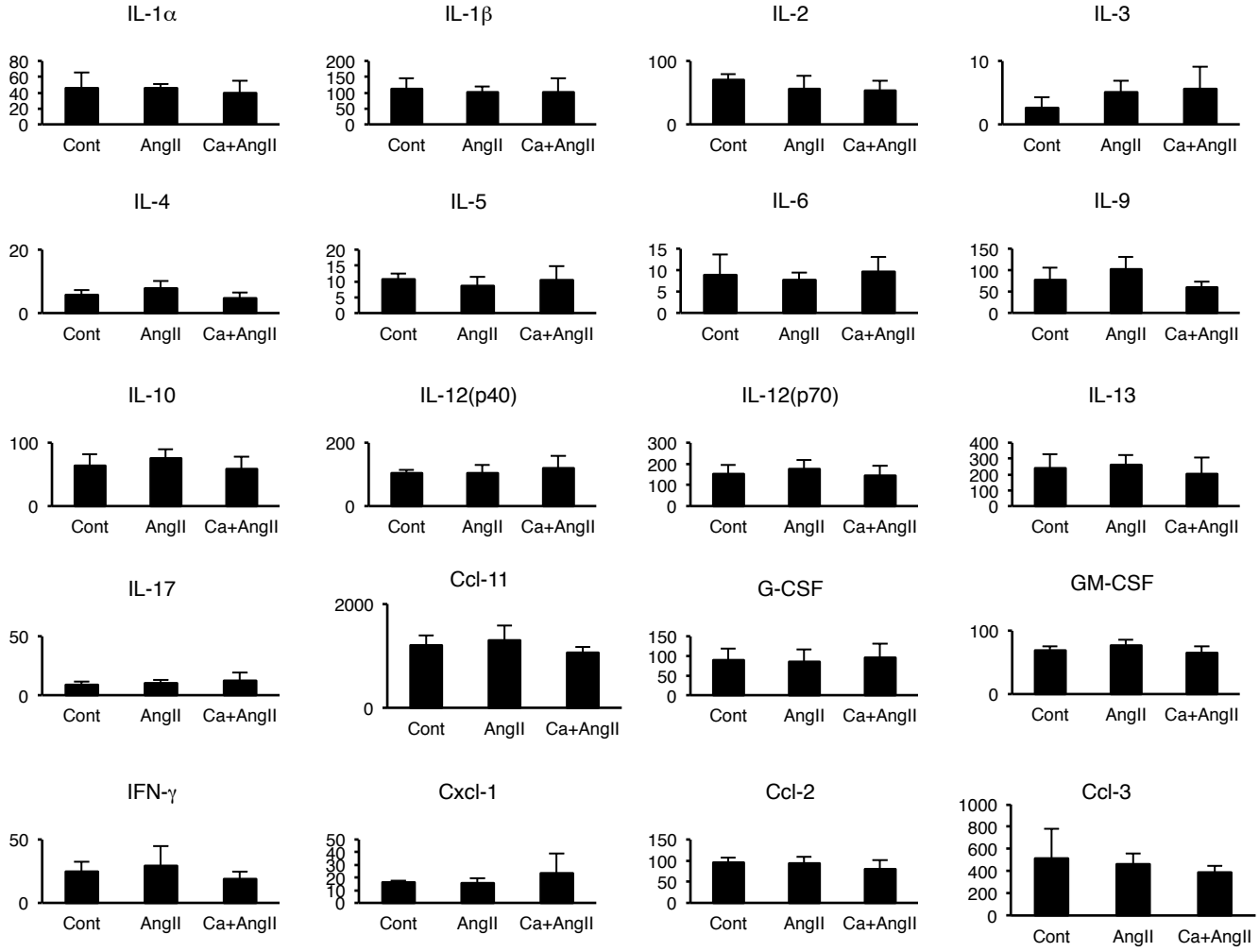


**Supplementary Figure 3**

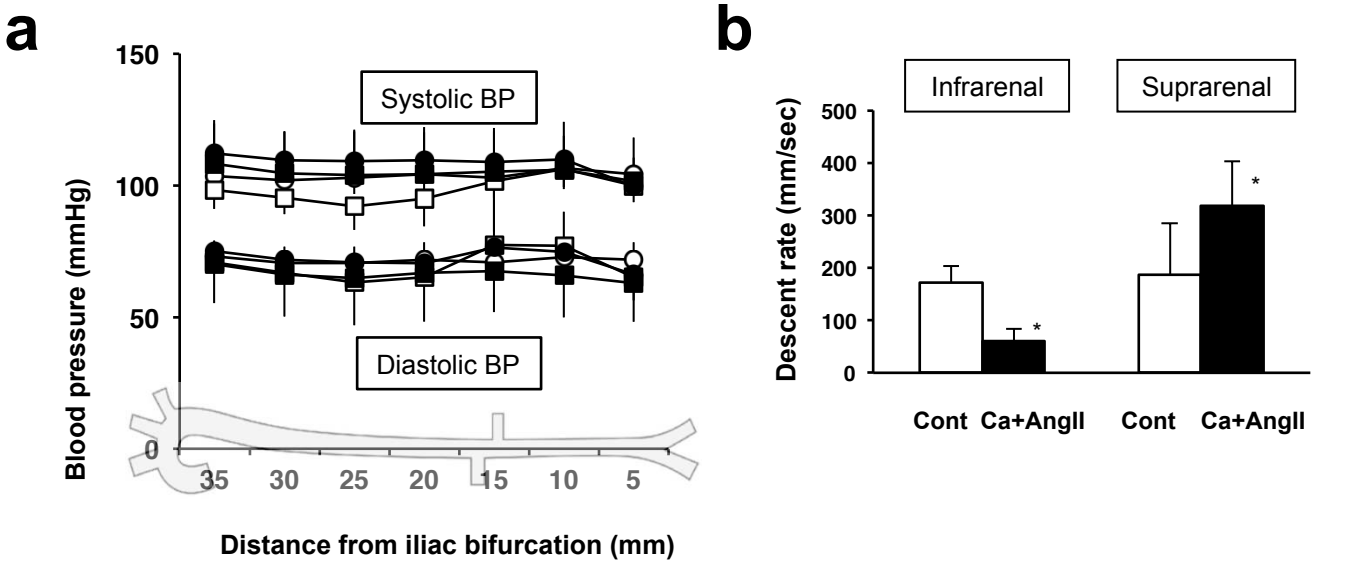


**Supplementary Figure 4**

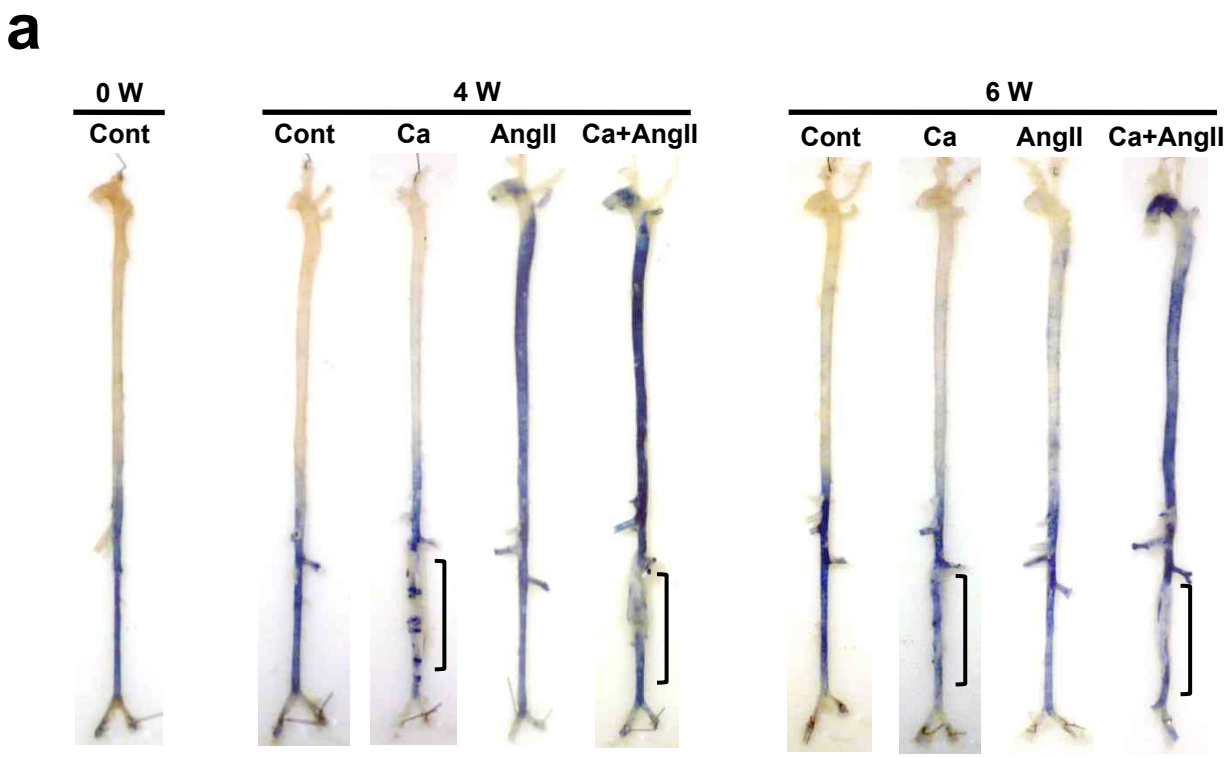


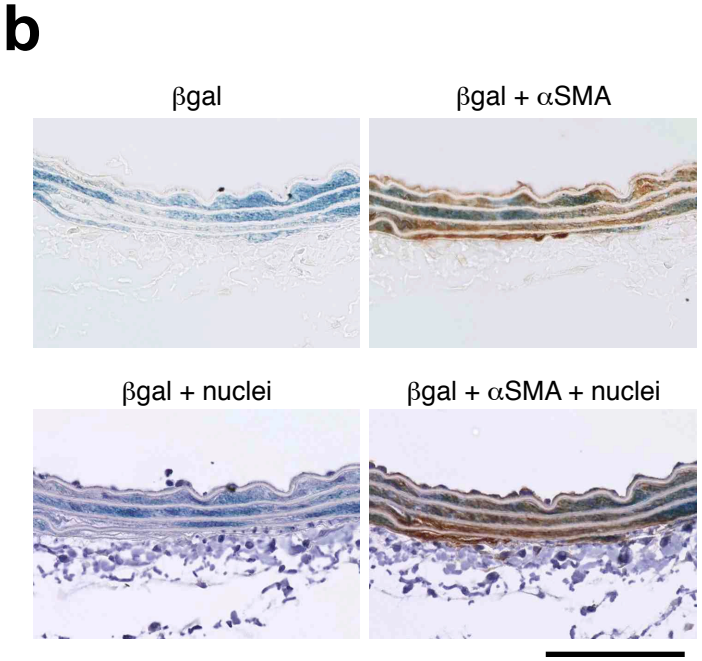


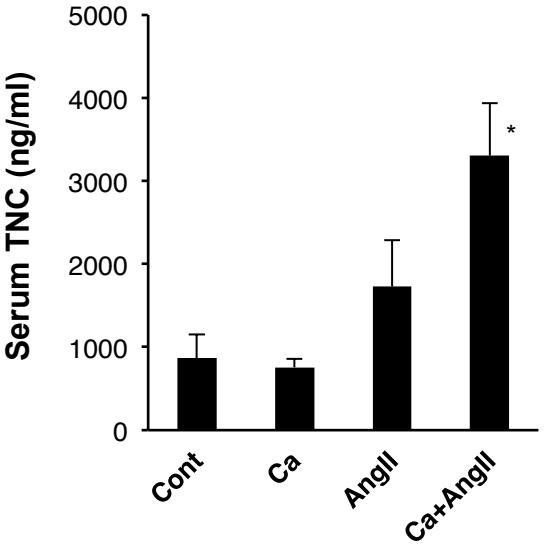


**Supplementary Figure 5**

**a**

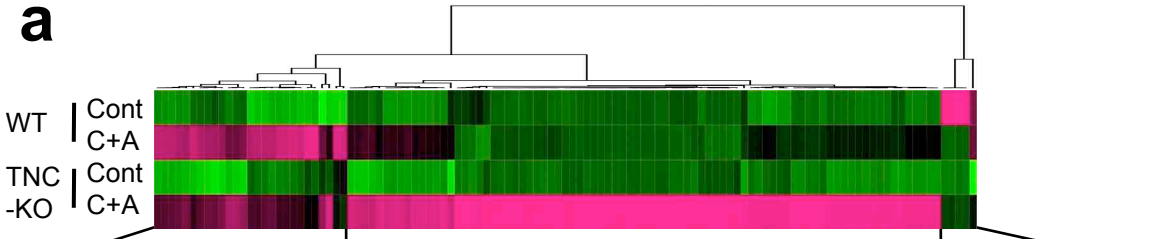


| subcluster #1 | | subcluster #2 | | | | | subcluster #3 | |
|---|---|---|---|---|---|---|---|---|
| Igfbp4 | Ngfr | Trf | Mefv | Ccl7 | Fgr | Pf4 | Myh1 | Myh1 |
| Serping1 | C2 | Anxa8 | Samhd1 | Il6 | Ccl3 | Hif1a | Myh1 | Myh2 |
| Igfbp4 | Saa2 | Anxa8 | Itgb2 | Ccl2 | Ncf1 | Hbegf | | Gja1 |
| C4b | Saa1 | Rtn4rl2 | Ccr1 | Gp9 | Nfkbiz | Fcer1g | | |
| Cd163 | Saa1 | Fn1 | Cxcl1 | Il1b | F5 | C5ar1 | | |
| Igfbp4 | Clec2d | Sphk1 | Tlr2 | Cxcl2 | Fcgr1 | Thbs1 | | |
| C1qb | Slc7a2 | Serpina3n | F10 | Cxcl3 | Alox5 | Selp | | |
| C1qb | Mecom | Ccr2 | Cd44 | Ncf1 | Rsad2 | Thbd | | |
| C1qa | Dhx58 | Saa3 | Ccl24 | Cxcl5 | Tlr6 | Procr | | |
| Lbp | Ccl12 | Fcgr2b | Thbs1 | Ccr1 | Rsad2 | Fcgr2b | | |
| Cfh | P2rx7 | Fcgr2b | Ccl4 | Arg1 | Fcgr3 | Ccr5 | | |
| F13a1 | Gatm | Fcgr2b | Slc11a1 | Chi3l3 | Olr1 | Tlr4 | | |
| Ccl8 | | Selp | Cd14 | Plek | Thbs1 | Il1r1 | | |
| S1pr3 | | Ccr5 | Plek | Chi3l3 | Tlr13 | C5ar1 | | |
| C2 | | Selp | Clec7a | Il18rap | Tfpi2 | | | |
| | | Cxcl1 | Plaur | Cd44 | Tlr4 | | | |
| | | Fgr | Cxcl1 | Plek | Hif1a | | | |

**Annotation Cluster 2** Enrichment Score: 24.71
GOTERM_BP_FAT GO:0009611~response to wounding
GOTERM_BP_FAT GO:0006954~inflammatory response
GOTERM_BP_FAT GO:0006952~defense response

**b**

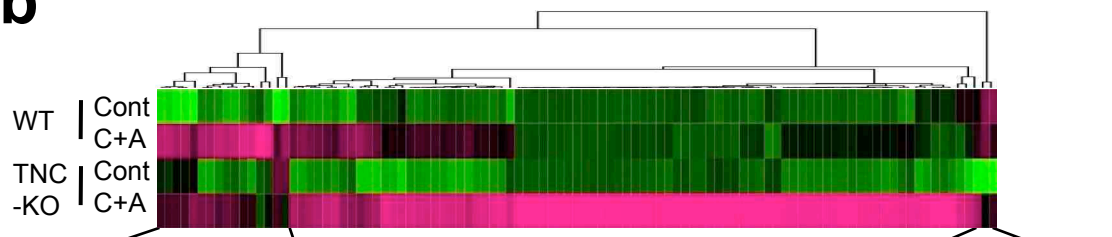


| subcluster #1 | | subcluster #2 | | | | | subcluster #3 |
|---|---|---|---|---|---|---|---|
| Spnb4 | Slit3 | Ednrb | Npas2 | Cxcl5 | Il11 | Hbegf | Gja1 |
| Itga6 | Ren1 | Tshr | Itga5 | Ccr1 | Cxcr2 | Fcer1g | Egr1 |
| Tns3 | Cyp11a1 | Ednrb | Ctgf | Csf3 | Il1f9 | Il33 | |
| Reln | Chl1 | Itga5 | Plat | Csf3r | Cxcl14 | Hif1a | |
| Chl1 | Calb1 | Cysltr1 | C3ar1 | Osm | Itgam | Spp1 | |
| Enpep | | Eps8 | C3ar1 | Fpr2 | Itgb2 | Runx1 | |
| Mmp14 | | Plau | Selp | Csf2 | Cela2a | Pvr | |
| Slit2 | | Lbp | C5ar1 | Ccr1 | Hif1a | Bdnf | |
| Ngfr | | Ccl8 | Ccl12 | Cxcl1 | Ccl6 | Runx1 | |
| Agt | | Wnt2 | Il6 | Ccl24 | Pf4 | Cxcl1 | |
| | | Pou3f2 | Ppbp | Ccl4 | Ccl9 | Pvr | |
| | | Cxcl14 | Cxcl1 | Lif | Ccl6 | Egfr | |
| | | Selp | Ccl7 | Ccl3 | C5ar1 | Egr2 | |
| | | Runx1 | Il1b | S100a9 | Selp | Lama5 | |
| | | Eps8 | Ccl2 | S100a8 | Fcgr3 | | |
| | | Itga5 | Cxcl2 | Fpr1 | Pdpn | | |
| | | C3ar1 | Cxcl3 | Tnfsf14 | Ccl9 | | |

**Annotation Cluster 3** Enrichment Score: 20.08
GOTERM_CC_FAT GO:0044421~extracellular region part
GOTERM_CC_FAT GO:0005578~proteinaceous extracellular matrix
GOTERM_CC_FAT GO:0031012~extracellular matrix

**Supplementary Figure 6a,b**

**c**

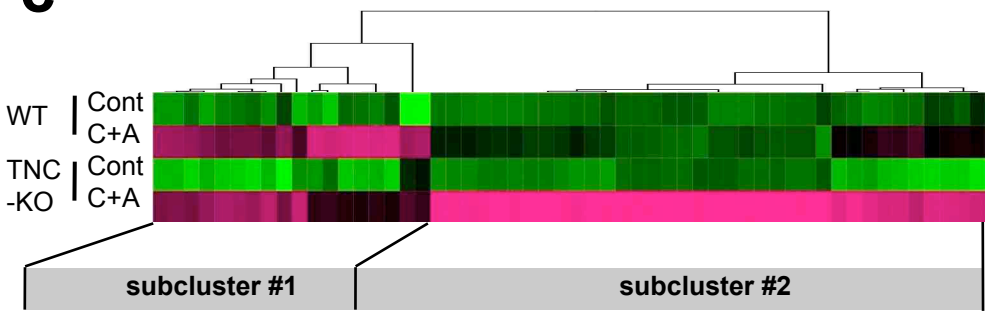


| | | | | | | | | | | | |
|---|---|---|---|---|---|---|---|---|---|---|---|
| Clec10a | Fbln7 | | Selp | Olr1 | | Clec5a | | Ctgf | | | |
| Clec11a | Clec2d | | Thbs1 | Tnfaip6 | | Cd44 | | Itih4 | | | |
| Fbn1 | Col5a1 | | Hbegf | Ccl7 | | Clec7a | | Cd93 | | | |
| Cd209a | Comp | | Lgals3 | Clec4d | | Thbs1 | | Gfpt2 | | | |
| Cfh | Clec4a2 | | Klra2 | Clec4e | | Ptx3 | | Fgf2 | | | |
| Clec4a3 | Col5a1 | | Clec4e | Clec4n | | Clec1b | | Selp | | | |
| Ccl8 | Gpnmb | | Thbs1 | Chi3l3 | | Fn1 | | | | | |
| Mrc1 | Col5a3 | | Itgam | Cd44 | | Sele | | | | | |
| Cd209f | | | Prg4 | Cd44 | | Selp | | | | | |
| Smoc2 | | | Pf4 | Clec4n | | Clec4a2 | | | | | |

**Annotation Cluster 4** Enrichment Score: 10.37

| | | | |
|---|---|---|---|
| GOTERM_BP_FAT | GO:0042330~taxis | GOTERM_MF_FAT | GO:0005125~cytokine activity |
| GOTERM_BP_FAT | GO:0006935~chemotaxis | GOTERM_BP_FAT | GO:0007610~behavior |
| GOTERM_MF_FAT | GO:0008009~chemokine activity | GOTERM_BP_FAT | GO:0030593~neutrophil chemotaxis |
| GOTERM_MF_FAT | GO:0042379~chemokine receptor binding | GOTERM_BP_FAT | GO:0016477~cell migration |
| GOTERM_BP_FAT | GO:0060326~cell chemotaxis | GOTERM_BP_FAT | GO:0048870~cell motility |
| GOTERM_BP_FAT | GO:0030595~leukocyte chemotaxis | GOTERM_BP_FAT | GO:0051674~localization of cell |
| GOTERM_BP_FAT | GO:0050900~leukocyte migration | GOTERM_BP_FAT | GO:0006928~cell motion |
| GOTERM_BP_FAT | GO:0007626~locomotory behavior | | |

**d**

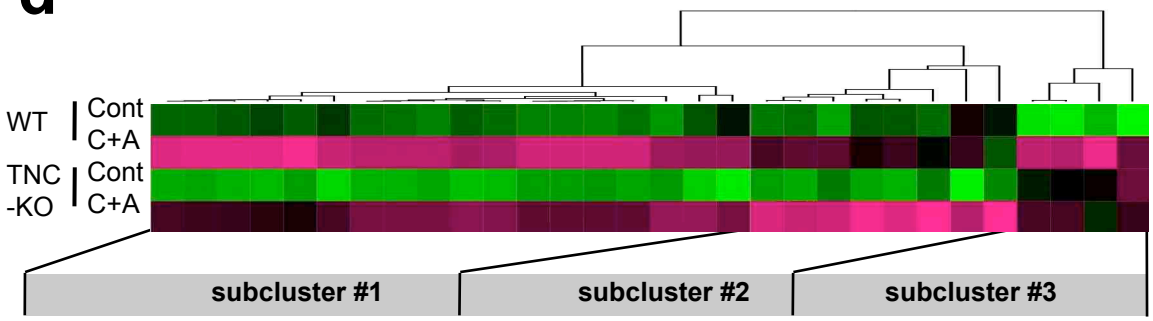


| | | | | | | | | | | | |
|---|---|---|---|---|---|---|---|---|---|---|---|
| Col8a1 | Col5a2 | Col1a1 | | Lox | Trf | | | Nid2 | | | |
| Col1a1 | Col4a2 | Fbln1 | | Lox | Timp1 | | | Col5a3 | | | |
| Col5a1 | Col5a2 | Col1a2 | | Smoc2 | Lama5 | | | Col11a1 | | | |
| Col5a1 | Fbn1 | Fbln1 | | Fn1 | Lox | | | Col11a1 | | | |
| Col8a1 | Eln | Col3a1 | | | | | | | | | |
| Col8a1 | Col4a1 | Eln | | | | | | | | | |

**Annotation Cluster 5** Enrichment Score: 7.86

| | |
|---|---|
| GOTERM_MF_FAT | GO:0030246~carbohydrate binding |
| GOTERM_MF_FAT | GO:0001871~pattern binding |
| GOTERM_MF_FAT | GO:0030247~polysaccharide binding |
| GOTERM_MF_FAT | GO:0005539~glycosaminoglycan binding |
| GOTERM_MF_FAT | GO:0008201~heparin binding |

**Supplementary Figure 6c, d**

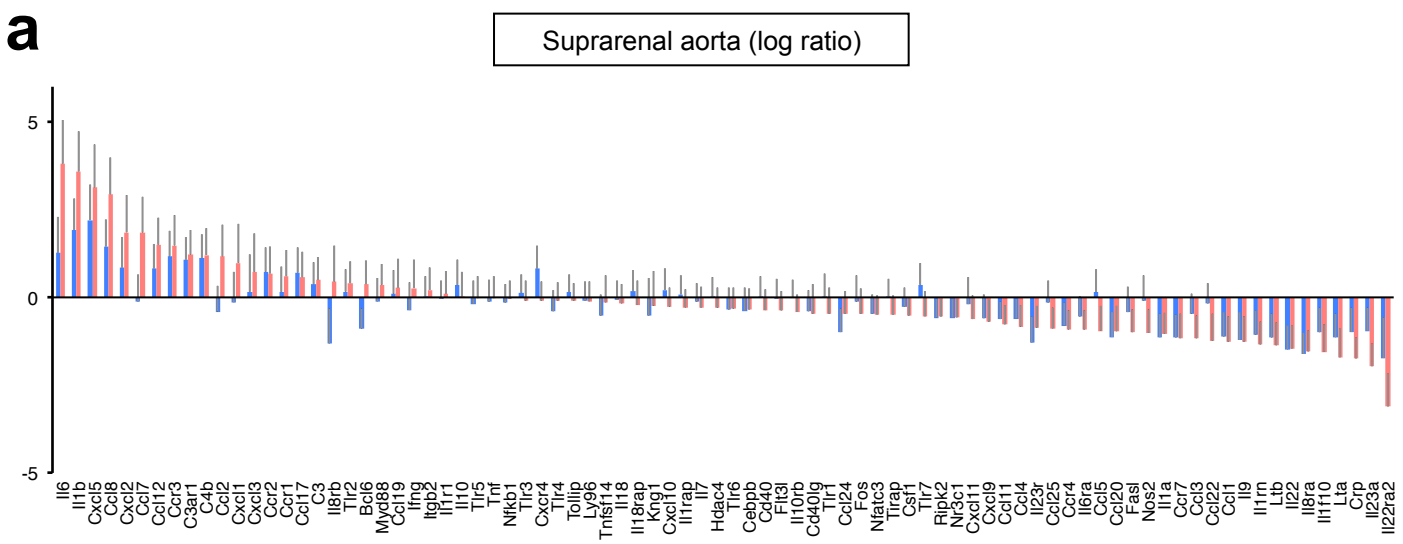


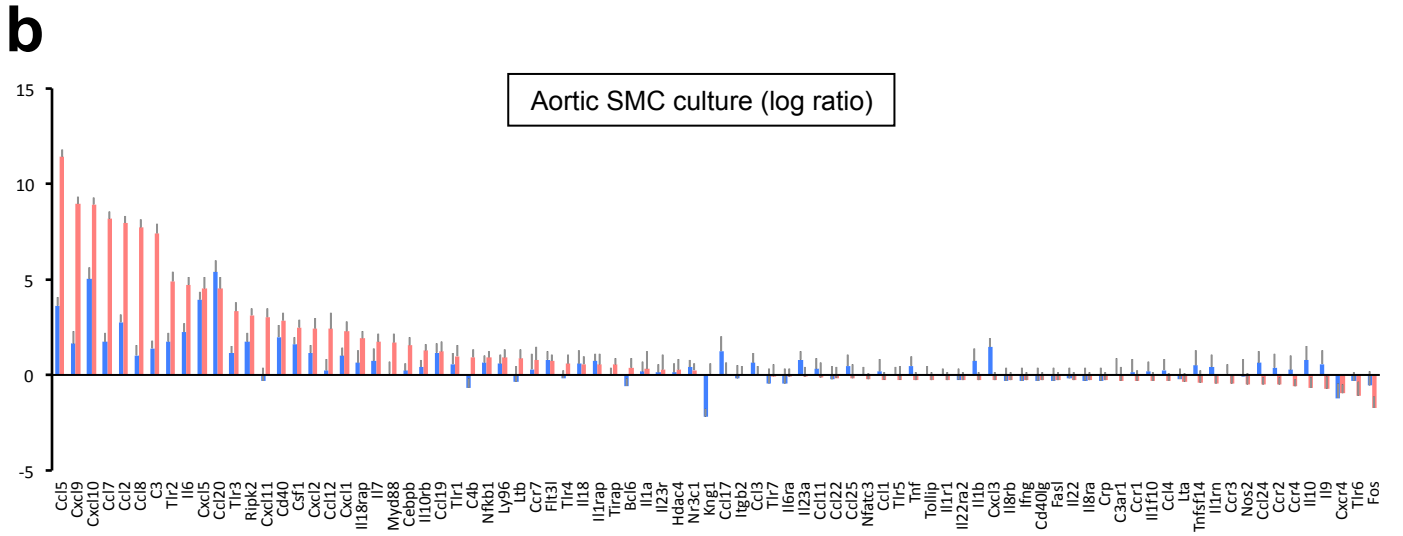


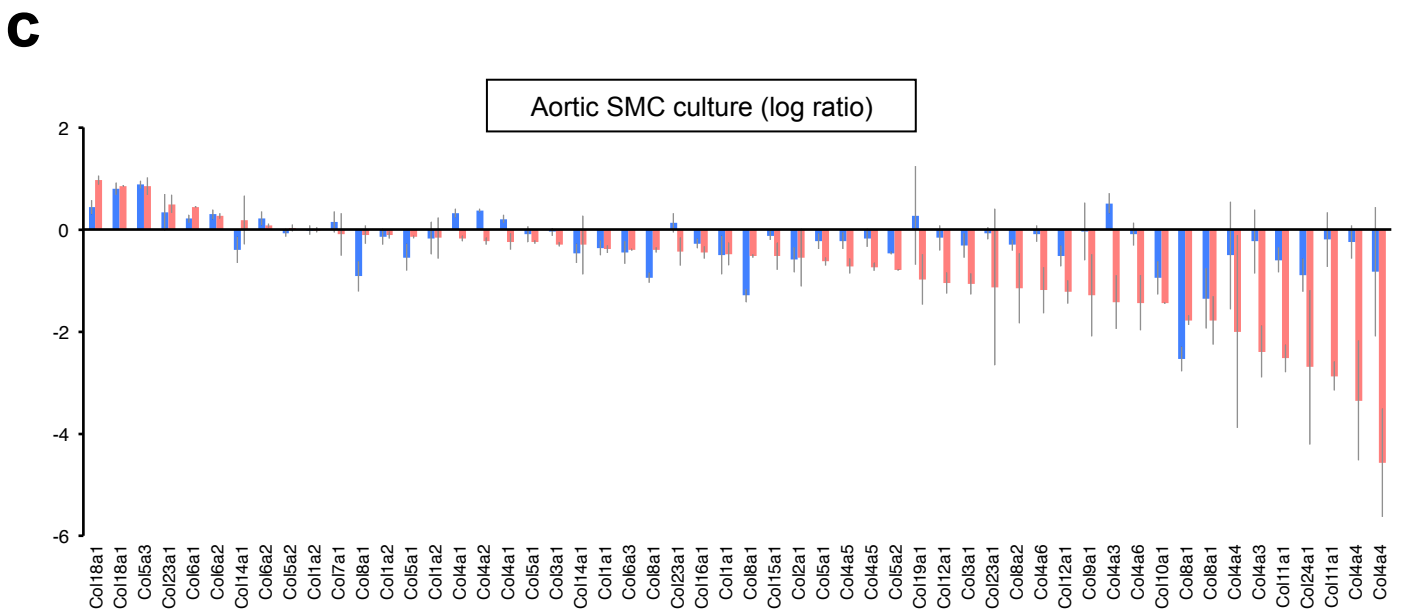


**Supplementary Figure 7**

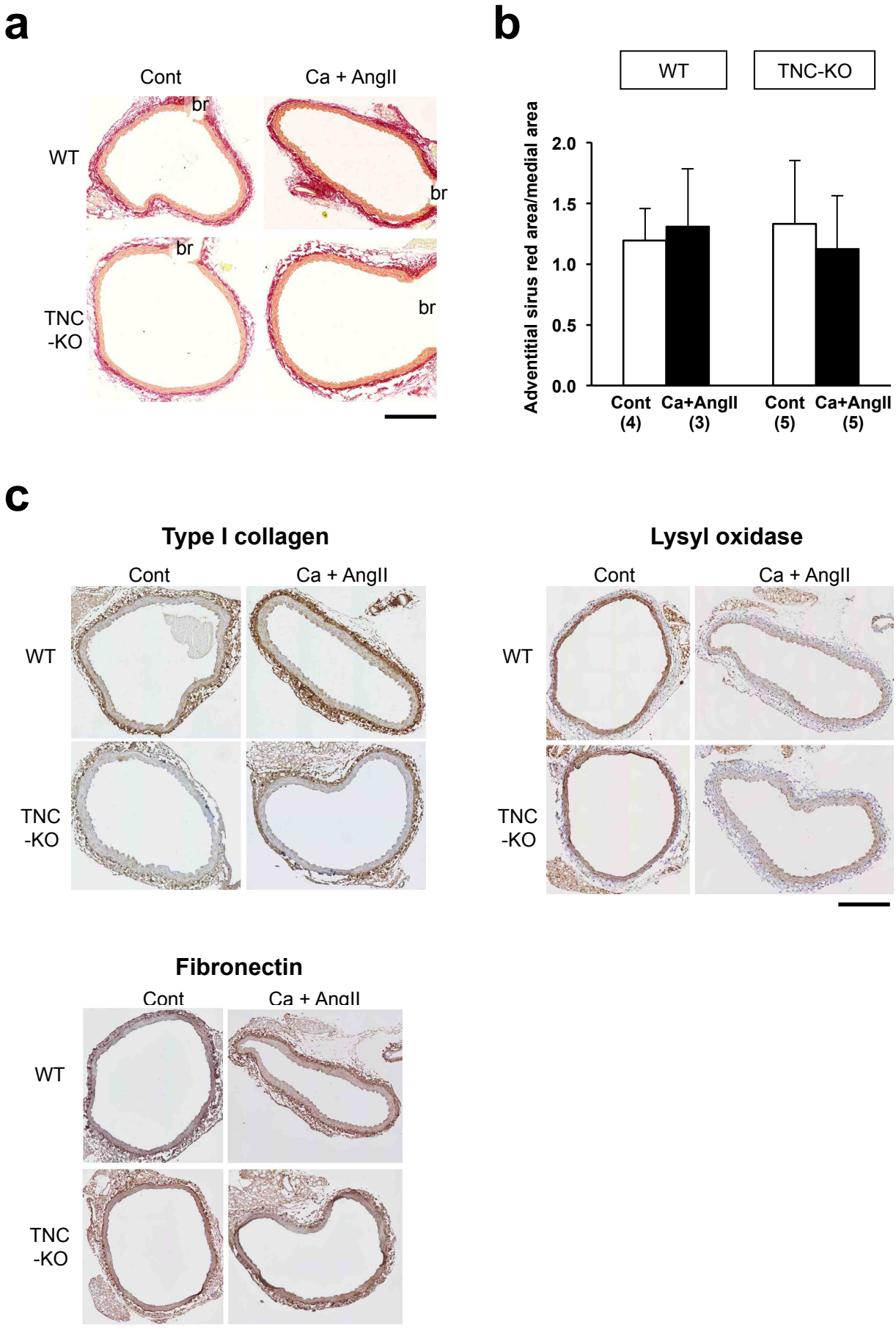


**Supplementary Figure 8**

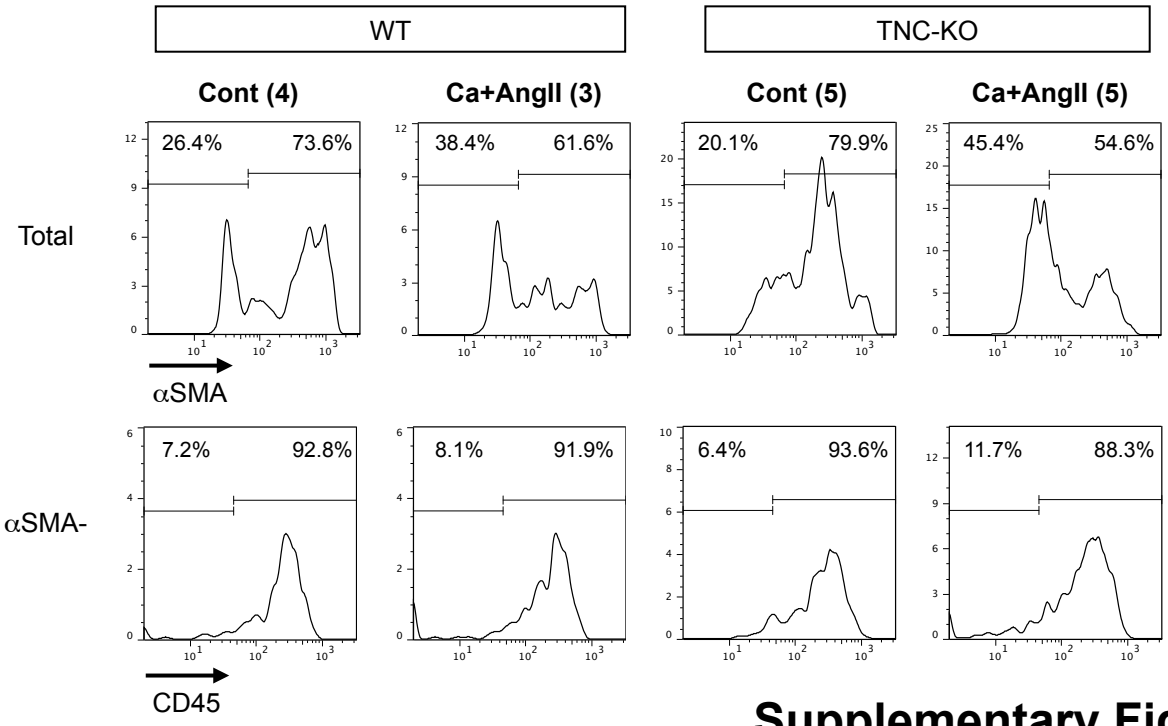


**Supplementary Figure 9**

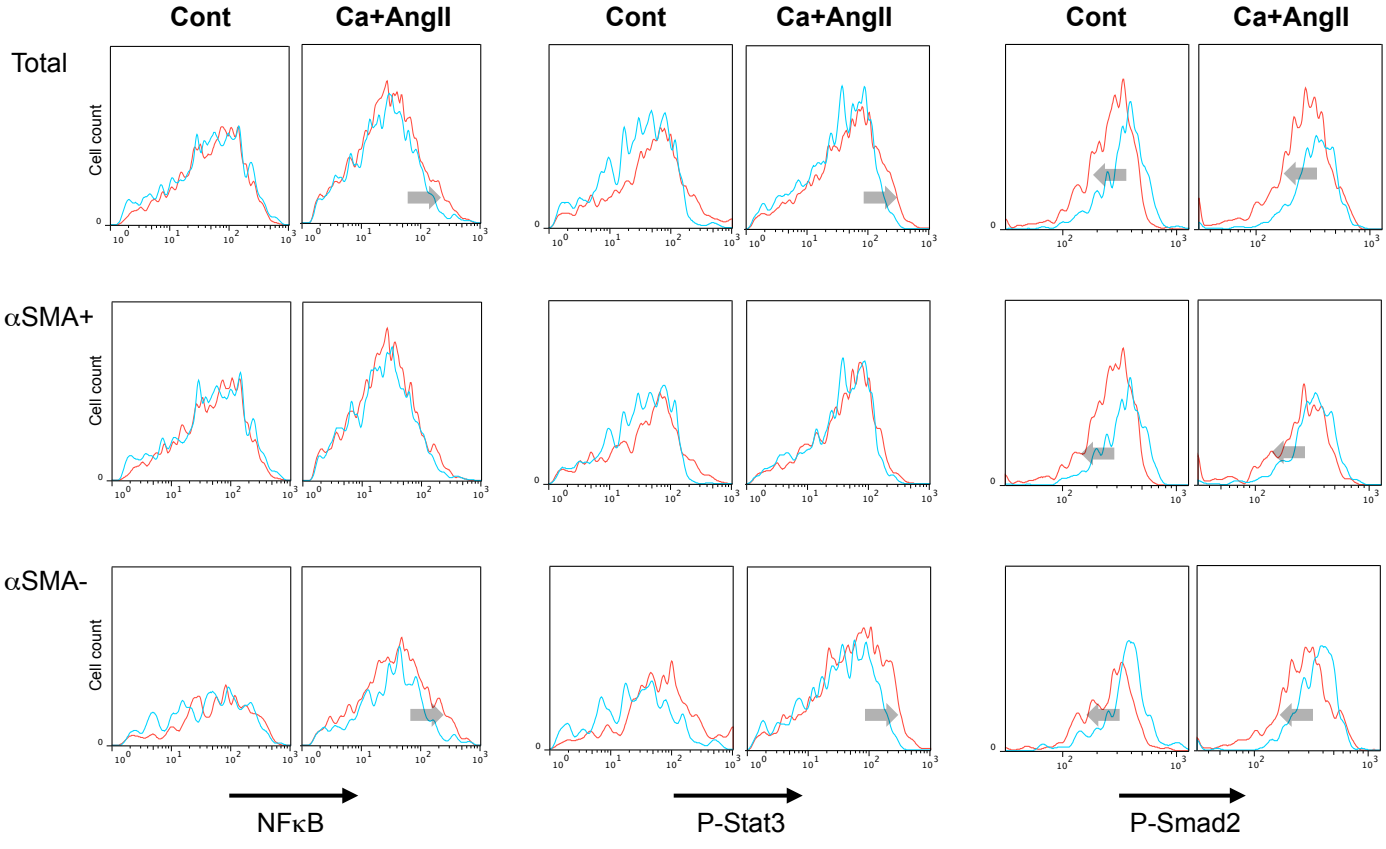


**Supplementary Figure 10**